

# The complex structure of the reconnecting magnetopause

F. S. Mozer,<sup>a)</sup> T. D. Phan, and S. D. Bale

*Physics Department and Space Sciences Laboratory, University of California, Berkeley, California 94720*

(Received 18 November 2002; accepted 5 March 2003)

Electric and magnetic fields observed in a one-of-a-kind example of a Polar satellite magnetopause crossing are consistent with static guide magnetic and electric fields, Hall magnetohydrodynamic (MHD) electric and magnetic fields, and a Z-component of the magnetic field that varied from  $-80$  nT to  $+80$  nT across the magnetopause [F. S. Mozer, S. D. Bale, and T. D. Phan, *Phys. Rev. Lett.* **89**, 015002 (2002)]. In spite of this excellent agreement with simulations, other features of the data were unanticipated. An empirical model, based on these measured fields and the assumption that the parallel electric field was zero, is developed to explain such features by showing that (1) Postreconnection  $\mathbf{E} \times \mathbf{B}/B^2$  flows, carrying electrons, magnetic field lines, and Poynting flux towards the X-line rather than away from it, occur at some locations. (2) The model and measured tangential electric fields varied significantly through the magnetopause. If the magnetopause was a time stationary structure, Faraday's law requires that it be three-dimensional on a spatial scale in the Y-direction of a few ion skin depths. This three-dimensionality may explain why only one example having fields that agree with Hall MHD simulations has been found. (3) There were regions within the magnetopause where electromagnetic energy may have been generated (in the normal incidence frame tied to the magnetopause). (4) Significant conversion of electromagnetic energy can occur inside the magnetopause in the absence of an electron diffusion region, parallel electric fields, or the electrons being decoupled from the magnetic field. It is emphasized that these properties are consequences of the Hall MHD and guide electric and magnetic fields in the absence of any additional non-MHD processes. © 2003 American Institute of Physics.  
[DOI: 10.1063/1.1570419]

## I. INTRODUCTION

Magnetic field reconnection is a process that both converts magnetic energy to particle energy and that modifies the magnetic field topology by connecting previously independent magnetic field lines. It occurs in laboratory plasmas as well as on the sun and other astrophysical objects, and it is the primary mechanism for providing energy to the plasma in the terrestrial magnetosphere. The microphysics of the reconnection process are being studied in the lab, by computer simulations and in the magnetosphere with data from satellites.

Two-dimensional static models of reconnection in the absence of guide fields show the presence of a Hall magnetohydrodynamic (MHD) electric field pointing towards the magnetopause from both sides and a Hall magnetic field component tangential to the magnetopause surface.<sup>1–5</sup> Magnetic fields consistent with the Hall effect have been reported at the magnetopause<sup>6,7</sup> and in the magnetotail.<sup>8,9</sup> A Polar satellite magnetopause crossing in the vicinity of the subsolar point, on 1 April 2001,<sup>10</sup> also revealed the Hall MHD magnetic field, as well as a Hall MHD electric field, while the magnetic field changed from 80 nT southward in the magnetosheath to 80 nT northward in the magnetosphere. The ions were decoupled from the magnetic field within the six-ion-skin-depth width of the crossing and the Hall MHD fields were in quantitative agreement with computer simulations. It

is emphasized that this is an almost unique diffusion region crossing in the database of  $\sim 1000$  crossings, for reasons that are discussed below.

## II. THE MODEL

Even with its many expected features, the April 1 crossing also displayed unexpected properties. One such set of properties is illustrated in Fig. 1, which gives the three components of  $\mathbf{E} \times \mathbf{B}/B^2$  measured during the magnetopause crossing of interest. The coordinate system of this figure is fixed to the magnetopause with the magnetosheath plasma incident on the magnetopause in the normal direction.  $X$  is in the maximum (minimum) variance direction of the electric (magnetic) field, pointing approximately sunward, and  $Z$  is in the minimum (maximum) variance direction of the electric (magnetic) field, pointing approximately northward in the ecliptic-normal direction. Each of the panels contains three curves which give the measured quantity and the standard deviations of that quantity associated with  $\pm 1$  mV/m and  $\pm 1$  nT measurement uncertainties in the electric and magnetic fields, respectively. (Uncertainties of the fields due to uncertainties in the minimum variance direction are small compared to the size of the guide fields, as has been verified by comparing minimum variance of  $B$ , maximum variance of  $E$ , and Faraday residue methods.<sup>10</sup>) In this plot, time runs from right to left, placing the magnetosphere at the left of the plot and the magnetosheath at the right. Near 0547:08 in Fig. 1, the uncertainties in the flow components are large because

<sup>a)</sup>Electronic mail: fmozer@sunspot.ssl.berkeley.edu

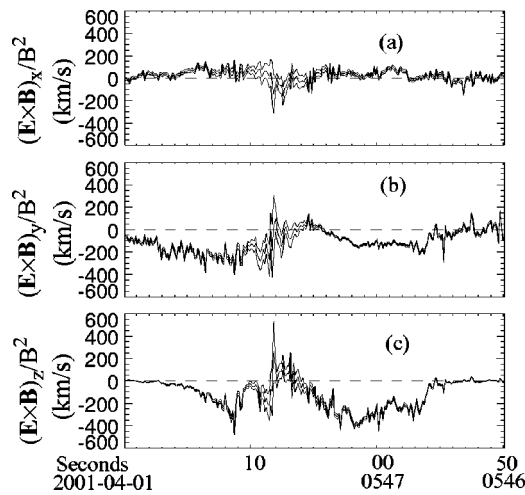


FIG. 1. Measured components of  $\mathbf{E} \times \mathbf{B}/B^2$  in the minimum variance coordinate system fixed to the magnetopause. Note that time runs backwards such that the magnetosphere is at the left boundary of the plots and the magnetosheath is at the right boundary.

the magnetic field was small. Otherwise, the flows were well measured so the following general features of the flow cannot be explained as due to experimental error:

- (1)  $(\mathbf{E} \times \mathbf{B}/B^2)_X$  was generally negative near the magnetosheath, at the right of the plot, and positive near the magnetosphere near the left of the plot, in agreement with the expected flow towards the magnetopause from both sides. Because these flows were small compared to those in the Y- and Z-directions, the X-component of flow will be small compared to the other components in the model and plots that are developed below.
- (2)  $(\mathbf{E} \times \mathbf{B}/B^2)_Y$  was significantly different from zero, was small at the center of the crossing, and was larger on the magnetospheric side of the crossing than on the magnetosheath side.
- (3)  $(\mathbf{E} \times \mathbf{B}/B^2)_Z$  reversed sign from its expected negative value (because the spacecraft was south of the X-line) to a positive value near the middle of the crossing. In an earlier publication,<sup>10</sup> it was speculated that this post-reconnection flow towards the X-line might be an indication of the electron diffusion region because the electron perpendicular flow differed from this reversed flow by several standard deviations. Further inspection of the electron data has shown that electron measurements were not made at times critical to the reversed flow so the interpretation of the postreconnection flow towards the X-line as being an observation of the electron diffusion region has been dismissed.

In the following discussion, the measured fields are modeled analytically without invoking additional non-MHD physics beyond the Hall effect, in order to understand the extent to which the peculiar properties of the  $\mathbf{E} \times \mathbf{B}/B^2$  flows may be understood within the context of a Hall MHD magnetopause. It is assumed that the spacecraft passed through a static magnetopause at a constant velocity in the normal direction, that  $X/X_0$  in Fig. 2 runs from  $-1$  at the magne-

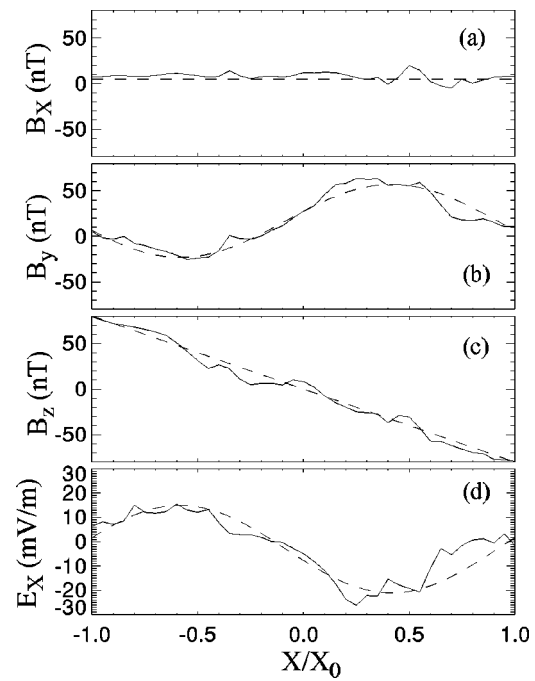


FIG. 2. Comparison of smoothed, measured, magnetic field components and  $E_X$  (the solid curves) with model fields described by Eqs. (1) (the dashed curves) for the same time period as that of Figs. 1 and 3.

sphere to  $+1$  at the magnetosheath, that the variations of the Hall MHD fields across the magnetopause are sinusoidal, and that  $B_Z$  varies linearly across the magnetopause. With these assumptions, the smoothed, measured,  $B_X$ ,  $B_Y$ ,  $B_Z$ , and  $E_X$  are fit in Fig. 2 by the model values (which are italicized),

$$B_X = B_N, \quad (1a)$$

$$B_Y = B_G + B_0 \sin(\pi X/X_0 + \varphi), \quad (1b)$$

$$B_Z = -B_A X/X_0, \quad (1c)$$

$$E_X = -E_0 \sin(\pi X/X_0 + \varphi) - E_G, \quad (1d)$$

where

$B_N$  = Normal magnetic field = 5 nT,

$B_G$  = Guide magnetic field in the Y-direction = 17 nT,

$B_0$  = Amplitude of the Hall magnetic field = 40 nT,

$B_A$  = Amplitude of the Z-component magnetic field = 80 nT,

$E_0$  = Amplitude of the Hall electric field = 18 mV/m,

$E_G$  = Guide electric field in the X-direction = 3 mV/m,

$\varphi = 15^\circ$ .

To complete the definition of the model fields along the spacecraft trajectory, it is assumed that both  $E_Z$  and the parallel electric field are zero. With these constraints,

$$E_Y = -E_X B_X/B_Y, \quad (2a)$$

$$E_Z = 0. \quad (2b)$$

Equation (2a) is shown to be consistent with the experimental data by plotting the measured  $E_Y$  and the measured  $-E_X B_X/B_Y$  in Fig. 3. Their general agreement attests to the fact that the measured parallel electric field was zero within

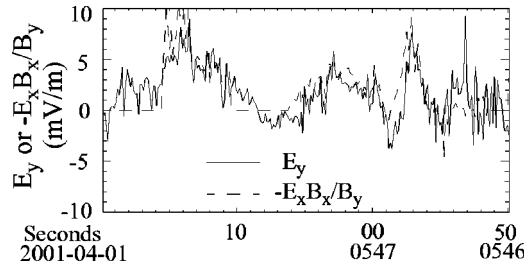


FIG. 3. Comparison of the measured  $Y$ -component of the electric field (solid curve) with  $-E_x B_x / B_y$  (the dashed curve) for the same time period as that of Figs. 1 and 2. Note that time runs backwards such that the magnetosphere is at the left boundary of the plot and the magnetosheath is at the right boundary.

experimental error through the portions of the crossing discussed in this paper. Their nonexact agreement is due in large measure to the fact that the experimental  $E_z$  was not exactly zero. The regions of zero data in the dashed curve of Fig. 3 occur where the magnitude of  $B_y$  was less than 12 nT and  $E_z$  was not equal to zero, hence, where  $-E_x B_x / B_y$  became unrealistically large.

The guide magnetic field, which is crucial to the understanding of unexpected features of the data, is visualized in Fig. 4, which presents a view of the asymptotic magnetic fields in the magnetosheath and magnetosphere, as viewed from the sun. The magnetic field differed by  $156^\circ$  in these two asymptotic regions. This angle was less than  $180^\circ$  because the guide magnetic field (the average field in the  $Y$ -direction) was nonzero. Hence, the model comparisons of magnetopause features with and without a guide magnetic field, which are discussed below, are really discussions of antiparallel and component merging.

Given the analytical expressions for the electric and magnetic fields along the spacecraft trajectory, the components of  $\mathbf{E} \times \mathbf{B} / B^2$  may be computed and compared with the smoothed, measured flows, as is done in Fig. 5. Because the measured flows are well explained in terms of the model fields, it is necessary to understand what properties of the model fields contribute to the facts that the post-reconnection

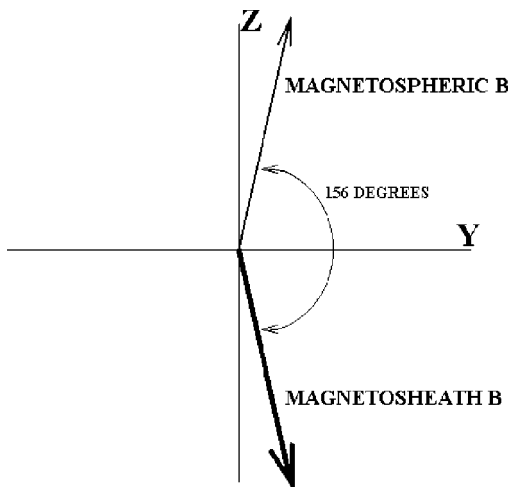


FIG. 4. The asymptotic magnetic fields in the magnetosheath and the magnetosphere as viewed from the sun.

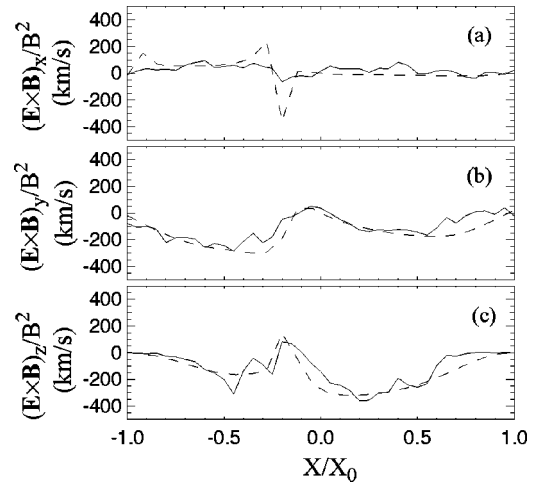


FIG. 5. Comparison of the smoothed, measured, components of  $\mathbf{E} \times \mathbf{B} / B^2$  (the solid curves) with the model values (the dashed curves).

flow is sometimes toward the  $X$ -line and that the  $Y$ -component of flow is variable. From the model,

$$(\mathbf{E} \times \mathbf{B} / B^2)_Z = (E_X B_Y + E_X B_X^2 / B_Y) / B^2 \\ = (E_X / B_Y) (B_X^2 + B_Y^2) / (B_X^2 + B_Y^2 + B_Z^2). \quad (3)$$

This expression can only be positive if  $E_X$  and  $B_Y$  have the same sign. From Eqs. (1b) and (1d) in the absence of the guide magnetic field,  $B_G$ , and the guide electric field,  $E_G$ ,  $E_X$  and  $B_Y$  are  $180^\circ$  out-of-phase so they do not have the same sign. However, due to the nonzero guide fields, there are regions where  $E_X$  and  $B_Y$  have the same sign and  $(\mathbf{E} \times \mathbf{B} / B^2)_Z$  is positive in these regions. Thus, the condition required for the postreconnection  $\mathbf{E} \times \mathbf{B} / B^2$  flow to be towards the  $X$ -line is the existence of Hall MHD electric and magnetic fields in the presence of either or both the guide electric and/or magnetic field.

Similarly,

$$(\mathbf{E} \times \mathbf{B} / B^2)_Y = -E_X B_Z / B^2. \quad (4)$$

The requirement that this flow component be different from zero and variable is the existence of the Hall MHD and guide  $E_X$  at the location of a nonzero  $B_Z$ .

Both the model and the measured tangential electric field vary with distance through the magnetopause (see Fig. 3). The model expression for this variation, obtained from Eqs. (1) and (2), is

$$\delta E_Y / \delta X = -[(E_G B_0 - E_0 B_G)(\pi B_N / X_0) \cos(\pi X / X_0 + \varphi)] / [B_G + B_0 \sin(\pi X / X_0 + \varphi)]^2. \quad (5)$$

The right-hand side of this equation is generally nonzero unless the guide fields  $E_G$  and  $B_G$  in the first term on the right are zero. For a steady state magnetopause, Faraday's law requires that  $E_X$  vary with  $Y$  as the negative of Eq. (5). For the measured guide fields,  $E_X$  varies by an amount greater than its measured value over a distance in the normally ignored  $Y$ -direction that is a few ion skin depths,  $c / \omega_{pi}$ . Thus, because of the presence of the guide electric and magnetic fields, the magnetopause is three-dimensional

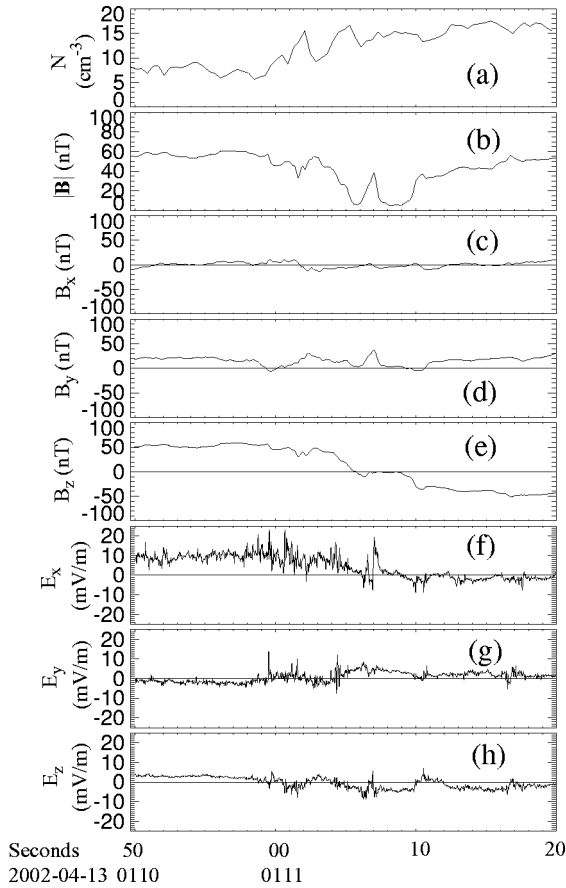


FIG. 6. Electric and magnetic fields measured during a 10 s crossing of the subsolar magnetopause on 13 April 2002, during which there was little indication of Hall MHD magnetic or electric fields.

over a short spatial scale and it would require a lucky trajectory to cross through it. This result may explain why only one observed magnetopause crossing among the  $\sim 1000$  events has Hall MHD electric and magnetic fields that agree with computer simulations.

The data of Fig. 6 are presented to emphasize the point that most magnetopause crossings do not exhibit Hall MHD electric and magnetic fields. This event was selected because of the similarity of many of its features to those of the crossing discussed in this paper.<sup>10</sup>  $B_z$  (panel e) varied from +50 nT in the magnetosphere to about -40 nT in the magnetosheath during the 10 s crossing. Because this change of  $B_z$  requires an important current in the  $Y$ -direction, the spacecraft must have passed through the ion diffusion region containing Hall MHD physics. The magnetic field decreased to a small value in the center of the crossing (panel b) while the density in the two asymptotic regions was the same within a factor of about 2. There was a guide magnetic field (panel d) of about 20 nT. In spite of these similarities to the event of interest, there is no indication of the bipolar  $B_y$  magnetic field (panel d) or  $E_x$  electric field (panel f) that is expected in the ion diffusion region from computer simulations. As mentioned above, this may be due to the three-dimensionality of the magnetopause.

One may consider what the  $\mathbf{E} \times \mathbf{B}/B^2$  flow in the model would be at other  $Z$ -distances within the magnetopause. At

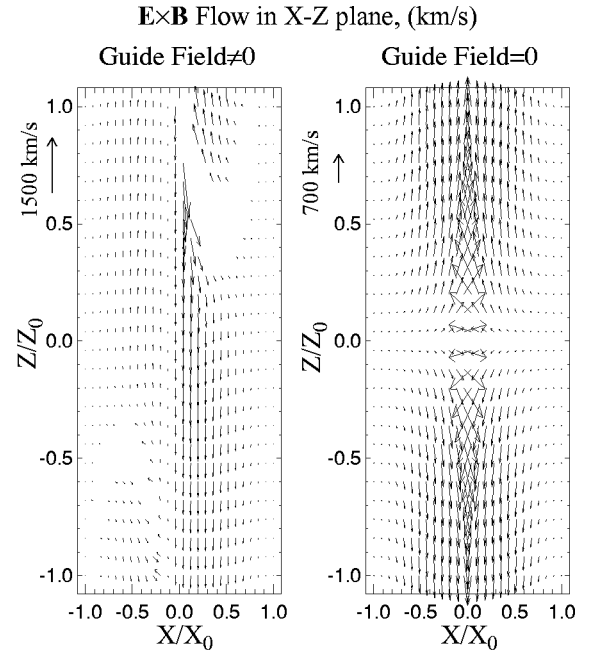


FIG. 7. The model  $\mathbf{E} \times \mathbf{B}/B^2$  flow in the  $X$ - $Z$  plane. The left panel includes the guide fields  $B_y = 17$  nT and  $E_x = 3$  mV/m. The right panel assumes that these guide fields are zero.

locations north of the  $X$ -line, the normal magnetic field component and the Hall component of  $B_y$  change sign. If it is assumed that the  $B_y$  guide field,  $B_G$ , also changes sign, then the values of the  $X$ - and  $Y$ -components of the model magnetic field north of the  $X$ -line are the negatives of those south of the  $X$ -line, so  $(\mathbf{E} \times \mathbf{B}/B^2)_z$  has the opposite sign north of the  $X$ -line. However,  $(\mathbf{E} \times \mathbf{B}/B^2)_x$  and  $(\mathbf{E} \times \mathbf{B}/B^2)_y$  would be the same north and south of the  $X$ -line.

There is no physical reason why the guide magnetic field should depend on the relative location north or south of the  $X$ -line. In fact, the more reasonable assumption is that this field is imposed externally, so it varies in the same way that  $B_y$  varies with  $Z$  in the magnetosheath. This means that the model  $B_G$  at locations other than that of the satellite is arbitrary. To consider how the magnetopause might look as a function of  $X$  and  $Z$ , it is assumed that  $B_G$  is constant, independent of  $Z$ . A linear dependence on  $Z$  of  $B_N$  and  $B_0$  is also assumed. With these assumptions, Eqs. (1) and (2) become

$$B_x = -B_N Z/Z_0, \quad (6a)$$

$$B_y = B_G - B_0(Z/Z_0) \sin(\pi X/X_0 + \varphi), \quad (6b)$$

$$B_z = -B_A X/X_0, \quad (6c)$$

$$E_x = -E_0 \sin(\pi X/X_0 + \varphi) - E_G, \quad (6d)$$

$$E_y = -E_x B_x/B_y, \quad (6e)$$

$$E_z = 0, \quad (6f)$$

where  $Z/Z_0$  varies from -1 at the location of the satellite crossing to +1 at a similar distance north of the  $X$ -line.

In the left panel of Fig. 7, the  $\mathbf{E} \times \mathbf{B}/B^2$  flow in the  $X$ - $Z$  plane, as computed from Eqs. (6), is given. As expected from the earlier discussion, the flow into the magnetopause across the  $X/X_0 = \pm 1$  boundaries is small compared to the other

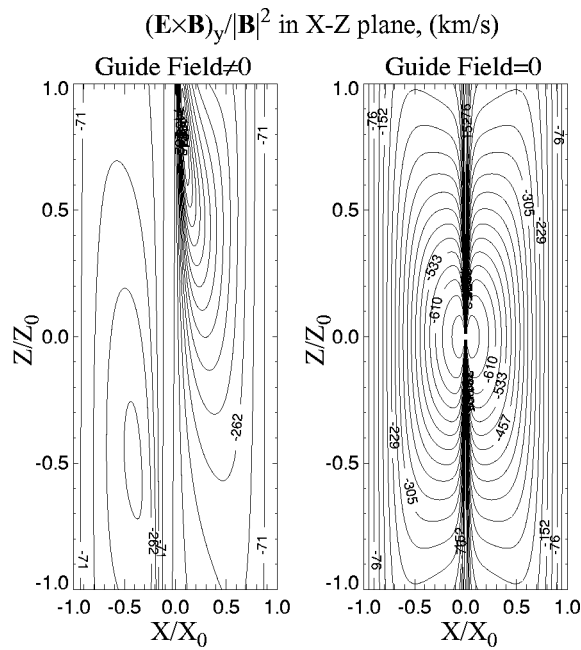


FIG. 8. The  $Y$ -component of  $\mathbf{E} \times \mathbf{B}/B^2$  in the  $X$ - $Z$  plane. The left panel includes the guide fields  $B_Y = 17$  nT and  $E_X = 3$  mV/m. The right panel assumes that these guide fields are zero.

component of the flow. The flow north (south) of the  $X$ -line is generally northward (southward) with regions of reversed flow in each half of the plane. Vortices in the flow are present and the spatial variation of the flow is significant.

In the right panel of Fig. 7, the flow is plotted from Eqs. (6) under the assumption that the guide fields,  $B_G$  and  $E_G$ , are zero. Under this assumption, the flow becomes that which is expected in static, two-dimensional models without guide fields. Namely, the flow is inward from the left and right and outward, as a jet, above and below the  $X$ -line. This is further proof that the complex flow with regions of post-reconnection flow towards the  $X$ -line are consequences of Hall MHD physics in the presence of guide fields.

In the left panel of Fig. 8, contours of  $(\mathbf{E} \times \mathbf{B}/B^2)_Y$  are presented. The flow is generally in the  $-Y$  direction and is as large as 1000 km/s. It is again emphasized that this spatially varying flow is different from that expected in conventional magnetopause models, and that this complexity is a natural consequence of the Hall MHD physics in the presence of guide fields.

In the right panel of Fig. 8, contours of  $(\mathbf{E} \times \mathbf{B}/B^2)_Y$  are presented for the case that the guide fields,  $B_G$  and  $E_G$ , are zero. The flow is symmetric in this case.

The current density may be calculated from the curl of the model magnetic field and dotted into the model electric field to produce the contour plots of  $\mathbf{j} \cdot \mathbf{E}$  given in the left panel of Fig. 9. In this figure,  $X_0 = 300$  km and  $Z_0$  is approximately  $X_0$  times the ratio of the asymptotic magnetic field to the normal magnetic field,<sup>11</sup> which is  $300B_A/B_N = 4800$  km. Surprisingly, the electromagnetic energy conversion is a minimum at the center of the magnetopause. It varies in space from about  $-1$  to  $+1$  W/km<sup>3</sup>.

As a result of the Hall MHD physics, electromagnetic energy may be gained as well as lost within the magneto-

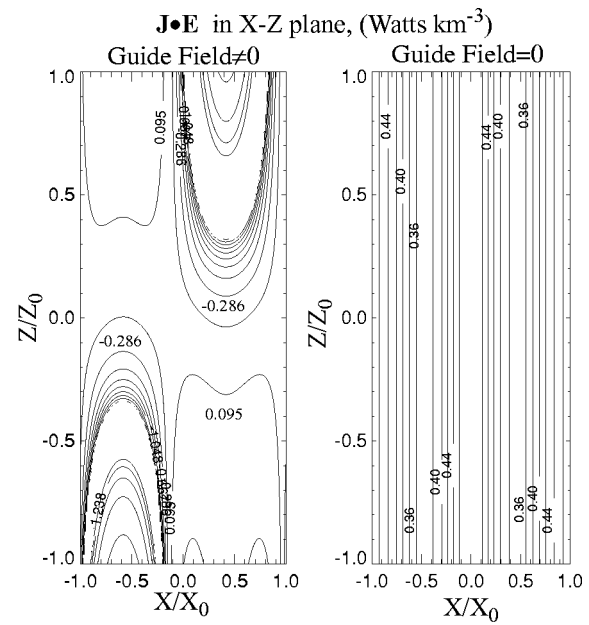


FIG. 9. Electromagnetic energy conversion in the  $X$ - $Z$  plane. The left panel includes the guide fields  $B_Y = 17$  nT and  $E_X = 3$  mV/m. The right panel assumes that these guide fields are zero.

pause (in the normal incidence frame tied to the magnetopause). In the magnetospheric (magnetosheath) side of the magnetopause, the Hall MHD  $B_Y$  has  $\delta B_Y/\delta Z > 0$  ( $\delta B_Y/\delta Z < 0$ ). This produces a negative (positive) current in the  $X$ -direction. This current, multiplied by the positive (negative) Hall MHD  $E_X$ , results in a negative component of  $\mathbf{j} \cdot \mathbf{E}$  in both halves of the magnetopause. This component can exceed the others to cause a net production of electromagnetic energy in some regions, as is evidenced in the left panel of Fig. 9.

The average value of  $\mathbf{j} \cdot \mathbf{E}$  over the surface of the left panel of Fig. 9 is about  $+0.05$  W/km<sup>3</sup>. Because this is sufficient power to accelerate  $10^8$  ions/cm<sup>2</sup>/s to several kV along the  $Z$ -axis, Hall MHD physics suffices to produce sufficient magnetic energy conversion to accelerate outflowing jets without an electron diffusion region, parallel electric fields, decoupling of electrons from the magnetic field, etc.

In the right panel of Fig. 9,  $\mathbf{j} \cdot \mathbf{E}$  is given for the case that the guide fields are zero. In this case, the electromagnetic energy conversion is relatively constant at about  $0.4$  W/km<sup>3</sup>.

It is emphasized that the detailed features exhibited in Figs. 7, 8, and 9 are model dependent, so they should not be interpreted quantitatively. However, the general results derived from the Hall MHD physics in the model are valid. These are that the  $\mathbf{E} \times \mathbf{B}/B^2$  flow in the  $X$ - $Z$  plane and the associated Poynting flux may be complex with postreconnection flows towards the  $X$ -line at some locations, that a large and complex  $\mathbf{E} \times \mathbf{B}/B^2$  flow in the  $Y$ -direction is expected, that significant electromagnetic energy may be converted within the magnetopause in regions where electrons are not decoupled from the magnetic field, and that the magnetopause has a three-dimensional structure on a spatial scale of a few ion skin depths.

- <sup>1</sup>B. U. Ö. Sonnerup, in *Solar System Plasma Physics*, edited by L. T. Lanzerotti, C. F. Kennel, and E. N. Parker (North-Holland, New York, 1979), Vol. III, pp. 45–108.
- <sup>2</sup>M. Hesse, J. Birn, and M. Kuznetsova, *J. Geophys. Res.* **106**, 3721 (2001).
- <sup>3</sup>M. A. Shay, J. F. Drake, B. N. Rogers, and R. E. Denton, *J. Geophys. Res.* **106**, 3759 (2001).
- <sup>4</sup>Z. W. Ma and A. Bhattacharjee, *J. Geophys. Res.* **106**, 3773 (2001).
- <sup>5</sup>P. L. Pritchett, *J. Geophys. Res.* **106**, 3783 (2001).
- <sup>6</sup>J. D. Scudder, P. A. Puhl-Quinn, F. S. Mozer, K. W. Ogilvie, and C. T. Russell, *J. Geophys. Res.* **104**, 19817 (1999).
- <sup>7</sup>X. H. Deng and H. Matsumoto, *Nature (London)* **410**, 557 (2001).
- <sup>8</sup>M. Oieroset, T. D. Phan, M. Fujimoto, R. P. Lin, and R. P. Lepping, *Nature (London)* **412**, 414 (2001).
- <sup>9</sup>T. Nagai, I. Shinohara, M. Fujimoto, M. Hoshino, Y. Saito, S. Machida, and T. Mukai, *J. Geophys. Res.* **106**, 25929 (2001).
- <sup>10</sup>F. S. Mozer, S. D. Bale, and T. D. Phan, *Phys. Rev. Lett.* **89**, 015002 (2002).
- <sup>11</sup>B. U. Ö. Sonnerup, G. Paschmann, I. Papamastorakis *et al.*, *J. Geophys. Res.* **86**, 10049 (1981).